JOURNAL OF VIROLOGY, Nov. 1991, p. 5828–5838
0022-538X/91/115828-11$02.00/0
Copyright © 1991, American Society for Microbiology
Vol. 65, No. 11

The 5′ Nontranslated Region of Hepatitis A Virus RNA: Secondary Structure and Elements Required for Translation In Vitro

EDWIN A. BROWN,* STEPHEN P. DAY, ROBERT W. JANSEN, AND STANLEY M. LEMON

Department of Medicine, The University of North Carolina at Chapel Hill, Chapel Hill, North Carolina 27599-7030

Received 13 March 1991/Accepted 23 July 1991

Although the lengthy 5′ nontranslated regions (5′NTRs) of other picornaviral RNAs form highly ordered structures with important functions in viral translation, little is known about the 5′NTR of hepatitis A virus (HAV). We determined the nearly complete 5′NTR nucleotide sequences of two genetically divergent HAV strains (PA21 and CF53) and included these data in a comparative phylogenetic analysis of the HAV 5′NTR. We identified covariant nucleotide substitutions predictive of conserved secondary structures and used this information to develop a model of the 5′NTR secondary structure, which was further refined by thermodynamic predictions and nuclease digestion experiments. According to this model, the 5′NTR comprises six major structural domains. Domains I and II (bases 1 to 95) contain a 5′-terminal hairpin and two stem-loops followed by a single-stranded and highly variable pyrimidine-rich tract (bases 96 to 154). The remainder of the 5′NTR (domains III to VI, bases 155 to 734) contains several complex stem-loops, one of which may form a pseudoknot, and terminates in a highly conserved region containing an oligopyrimidine tract preceding the putative start codon by 13 bases. To determine which structural elements might function as an internal ribosome entry site, RNA transcripts representing the HAV 5′NTR with progressive 5′ deletions were translated in rabbit reticulocyte lysates. The translation product was truncated, unprocessed P1 polyprotein. Removal of the 5′-terminal 354 bases of the 5′NTR had little effect on translation. However, deletion to base 447 slightly decreased translation, while deletion to base 533 almost completely abolished it. These data indicate that sequences 3′ of base 355 play an important role in the translation mechanism utilized by genomic-length HAV RNA. Significantly, this region shares several conserved structural features with the internal ribosome entry site element of murine encephalomyocarditis virus.

The RNA genome of hepatitis A virus (HAV), a medically important hepatotropic picornavirus, contains a highly conserved 5′ nontranslated region (5′NTR) approximately 730 nucleotides in length (7, 44). Very little is known concerning the specific functions of this 5′NTR, but mutations within this region of the genome have been demonstrated in several HAV variants that have been adapted to growth in cell culture (6, 20, 39). One of these mutations, a U-to-G substitution at base 687, has been shown to positively influence the growth of a cell culture-adapted variant in monkey kidney (BS-C-1) cells (8). Because the change in host range that accompanies adaptation of HAV to growth in monkey kidney cell cultures has been associated with reduced hepatovirulence in susceptible primates (5), mutations within the 5′NTR may be of relevance to viral attenuation. This hypothesis is further supported by abundant evidence that mutations within the 5′NTR of poliovirus, a picornavirus that is distantly related to HAV, play an important role in defining the attenuation phenotype of oral poliovirus vaccine strains (12, 33).

Recent studies with several other picornaviruses suggest that the 5′NTR of HAV should contain *cis*-acting elements involved in cap-independent translation of viral RNA (3, 19, 35, 45, 46). As might be expected, this function has been shown to be dependent on both primary and higher-order RNA structures. However, computerized algorithms which predict the secondary structure of RNAs on the basis of thermodynamic considerations alone are limited in their ability to correctly predict the structure of RNAs of this length (17). A phylogenetic approach involving a search among viruses of different serotypes for covariant nucleotide substitutions which predict conserved, helical structures has proven considerably more useful in developing models of the secondary structures of the 5′NTRs of enteroviruses, cardioviruses, and aphthoviruses (36–38, 41). Unfortunately, the nucleotide sequence of the HAV 5′NTR shows no homology with the 5′NTRs of these other picornaviruses, precluding the establishment of meaningful sequence alignments and the application of these models to the structure of the HAV 5′NTR. Moreover, comparative sequence analysis of available HAV 5′NTR sequences has not been possible because of the highly conserved nature of the 5′NTR nucleotide sequences of most human HAV strains.

Recently, however, several genetically divergent simian and human strains of HAV have been identified, and their genomes have been partially sequenced (4, 21). We report here the 5′NTR sequences of two of these genetically divergent viruses. By comparing the 5′NTR sequences of these and other HAV strains, we identified a number of covariant nucleotide substitutions which suggest the existence of conserved helical RNA domains. In this report, we describe a model of the secondary structure of the HAV 5′NTR which is based on the identification of these covariant nucleotide substitutions. The structure that we propose has been refined by the secondary application of thermodynamic modeling and by the results of experiments utilizing single- and double-strand-specific RNases to probe the structure of synthetic HAV RNA. These studies indicate that the HAV 5′NTR has several structural motifs in common with the aphthovirus and cardiovirus 5′NTRs (36).

Picornavirus RNAs do not have a 5′ m^7G cap structure (16, 32) and appear to utilize a mechanism of translation initiation which differs from the ribosomal scanning process

* Corresponding author.

TABLE 1. HAV 5′NTR oligodeoxynucleotide primers

Primer	Sequence
NA0373	CCTTGTGGAAGATCAAAGAG
NA0505	CTGGATGAGAGTCAGTCCTC
NA0594	TTTAAGGCCAAATGATGTTTGC
NA0642	GAACAGTCCAGCTGTCAATG
NA0671	TACCTCAGAGGCAAACACCACATAA
NA0765	TCAAGACCACTCCCAACAGT
PA0031	TCCCTCTTGGAAGTCCATGGTGAGGGGAC

involved in the translation of most eucaryotic mRNAs (23, 24). Several picornaviruses, including poliovirus, encephalomyocarditis virus (EMCV), and foot-and-mouth disease virus, contain within their 5′NTRs a *cis*-acting element which has been variably termed an internal ribosome entry site (IRES) or ribosomal landing pad (19, 35, 46). This element directs binding of the 40S ribosomal subunit to the viral RNA in a cap-independent fashion, resulting in initiation of translation downstream of multiple AUG triplets and hundreds of bases downstream of the 5′ terminus. This cap-independent mechanism of translation initiation permits viral translation to proceed efficiently in cells in which virus-specified proteins have promoted cleavage of the p220 cap-binding protein complex, effectively shutting down cap-dependent translation of cellular mRNAs (42). HAV differs from many other picornviruses in that infection does not shut down the translation of 5′-capped cellular mRNAs (14). However, as with other picornaviruses, the 5′NTR of HAV contains numerous AUG triplets prior to that which opens the reading frame encoding the polyprotein (AUG-11 in HAV strain HM175). This feature of its 5′NTR suggests that HAV follows a mechanism of translation initiation similar to that of other picornaviruses. To gain a better understanding of this mechanism, we examined the efficiency with which 5′-terminally truncated HAV RNAs are translated in rabbit reticulocyte lysates. These results, coupled with the proposed secondary structure model, suggest that the HAV 5′NTR contains an IRES element and has a basic functional organization like that of other picornaviruses.

MATERIALS AND METHODS

HAV 5′NTR nucleotide sequences. The PA21 and CF53 strains of HAV, which were recovered respectively from a naturally infected owl monkey in Panama and from an infected human in France, are genetically divergent from most human HAV isolates and represent distinct genotypes of HAV (21). We determined the nucleotide sequences of most of the 5′NTRs of these viruses by a combination of direct dideoxynucleotide sequencing of cDNA fragments amplified by an antigen capture/polymerase chain reaction method (21), using primers PA0031 and NA0765 (Table 1), and by dideoxynucleotide sequencing of selected cDNA clones from PA21 virus (4). We aligned these sequences with those published for five distinct human HAV strains: HM175 (wild type) (7), MBB (34), LA (30), CR326 (27), and HAS-15 (43). We added to this alignment the unpublished sequence of the human HAV strain KRM003, kindly provided to us by Y. Moritsugu and A. Nomoto, and the partial sequence of the simian strain AGM027, provided to us by S. Tsarev. Thus, the final sequence data base comprised the partial or complete 5′NTR sequences of seven human and two simian HAV strains, representing four distinct HAV genotypes (21). Because of a high degree of conservation, the alignment of these nucleotide sequences (Fig. 1) was straightforward in almost all regions.

Comparative sequence analysis. The sequence alignment was searched manually for covariant nucleotide substitutions, accepting both canonical (G · C and A · U) and noncanonical (G · U) base pairs, in order to identify potentially conserved helical structures within the 5′NTR (17). Substitutions were considered covariant and suggestive of helix formation only if they occurred in both strands of the helix (e.g., we did not consider G · C-to-G · U changes within potential helices as indicative of covariance). Helical structures were considered confirmed when covariant substitutions were identified within two or more different base pairs of the helix (17), although we indicate potential helices suggested by the occurrence of covariant substitutions within only a single base pair.

Thermodynamic modeling of the 5′NTR structure. Helical structures identified as described above were included as folding constraints on structural predictions made by the RNAFOLD program of Zucker and Stiegler, which is included in the University of Wisconsin Genetics Computer Group sequence analysis software package (10). Folding energies used in this program were those of Freier et al. (13). Additional predictions were made by the STAR program developed by Abrahams et al. (1). This program applies a unique algorithm which allows the prediction of some tertiary interactions, including RNA pseudoknots. STAR program predictions were used to resolve conflicts between the structures predicted by RNAFOLD and the results of the enzymatic analysis. The sequence used for construction of the final model was that of the wild-type HM175 virus (7).

Enzymatic analysis of RNA secondary structure. We used single- and double-strand-specific RNases to confirm the structures predicted by the analysis of covariant substitutions and to probe highly conserved regions of the 5′NTR in which a phylogenetic analysis was not possible. RNA was transcribed under direction of SP6 polymerase (Promega) from plasmid pAccI after it had been linearized with *Xmn*I. pAccI contains the 5′ 2,025 nucleotides of p16 HM175 virus (20) inserted into *Hin*dIII and *Acc*I sites of the vector pGEM/3zf(−) (Promega), downstream of the SP6 promoter. Reaction mixes contained 1 μg of RNA, 10 μg of tRNA (Boehringer Mannheim), and 0.2 to 0.5 U of RNase T_1, RNase V_1 (Pharmacia), or RNase T_2 (Bethesda Research Laboratories) in buffer A (10 mM Tris [pH 7.5], 10 mM $MgCl_2$, 50 mM KCl) or 50 U of S1 nuclease (Pharmacia) in buffer B (10 mM Tris [pH 7.5], 10 mM $MgCl_2$, 50 mM KCl, 1 mM $ZnSO_4$) in a total volume of 80 μl. The RNA was digested for 10 min at room temperature. Reactions were stopped by extraction with phenol after the addition of 10 μg of tRNA. A control aliquot taken before addition of RNase was processed simultaneously with the digested RNA. The aqueous phase was extracted with $CHCl_3$ and ethanol precipitated in 2 M ammonium acetate.

RNase cleavage sites were identified by primer extension with end-labelled oligonucleotide primers (Table 1). In a total volume of 5 μl, 1 pmol of ^{32}P-labelled primer was hybridized to 0.5 μg of digested RNA in RT buffer (50 mM Tris [pH 8.3], 8 mM $MgCl_2$, 50 mM KCl). The solution was heated to 90°C for 2 min, held at 65°C for 10 min, and slowly cooled to 42.5°C over 1 h. RT buffer (5 μl) containing 20 mM dithiothreitol, 3 U of avian myeloblastosis virus reverse transcriptase (Life Sciences), and 170 mM deoxynucleoside triphosphate was added, and the mixture was held at 42.5°C for 30 min (25). A sequencing ladder was prepared by using dideoxynucleotides, undigested RNA, and the same ^{32}P-

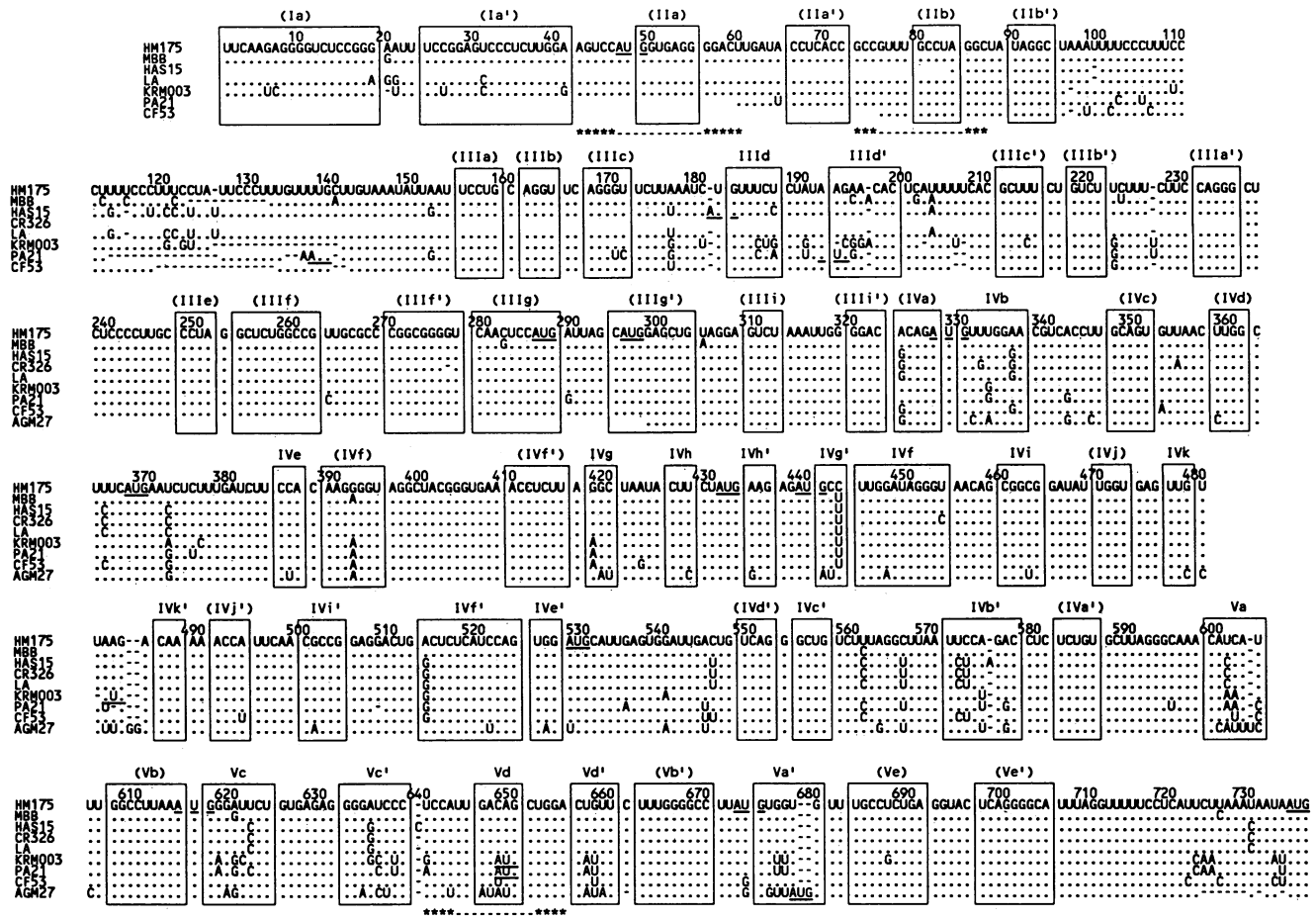

FIG. 1. Alignment of human and simian HAV 5'NTR sequences inclusive of nucleotides 1 through 737 (wild-type HM175 numbering). Dots indicate conserved bases (relative to the HM175 sequence); dashes indicate deletions. AUG triplets are underlined. Boxes indicate approximate locations of the proposed helical structures. From the 5' terminus, complementary sequences involved in potential helices are labelled sequentially by major domain (i.e., IIa, IIa'; IIb, IIb'; etc.). Potential helices that are not supported by the presence of covariant base substitutions have labels enclosed by parentheses. Base pairing in possible pseudoknots is indicated by the asterisks below the alignment.

labelled primer (15). The samples (enzymatically modified RNA, control reaction, and sequencing ladder) were electrophoresed through a 6% polyacrylamide gel, which was subsequently dried and exposed to Kodak X-Omat AR film (Eastman Kodak) for 4 to 16 h.

Synthesis of 5'-terminally deleted 5'NTR RNAs. To evaluate the roles that various regions of the 5'NTR play in controlling translation in vitro, we constructed multiple 5' deletion mutants from plasmid pAccI. Constructs pΔ46 (containing the p16 HM175 5'NTR sequence inclusive of bases 46 to 734), pΔ151 (bases 151 to 734), pΔ355 (bases 355 to 734), pΔ447 (bases 447 to 734), pΔ533 (bases 533 to 734), pΔ634 (bases 634 to 734), pΔ740 (which contains none of the 5'NTR sequence but includes bases 740 to 2024 of p16 HM175 virus), and pΔ745 (bases 745 to 2024) were made by digestion of pAccI with *Hin*dIII and *Nco*I, *Bsp*MI, *Hpa*I, *Eco*NI, *Nsi*I, *Bam*HI, *Afl*III, and *Xba*I, respectively, followed by blunt ending with the Klenow fragment of DNA polymerase and religation with T4 DNA ligase. The resulting plasmids were linearized within the multiple cloning site by *Eco*RI, and runoff transcripts were made under direction of SP6 RNA polymerase. The integrity and size of these synthetic RNAs were confirmed by formaldehyde-agarose gel electrophoresis (data not shown). The nucleotide numbering of these constructs is based on the sequence of wild-type HM175 virus (7).

In vitro translation of HAV RNA. Synthetic RNAs (200 μg/ml) were translated in nuclease-treated rabbit reticulocyte lysates (Promega) as suggested by the manufacturer. Aliquots of the ^{35}S-labelled translation products, representing a truncated, 48-kDa HAV P1 protein, were immunoprecipitated (see below) with rabbit preimmune serum to remove nonspecific antibody-antigen complexes. The samples were then incubated at 4°C overnight with a 1:100 dilution of rabbit antiserum to recombinant HAV VP0 (kindly provided by J. M. Johnston) or guinea pig antiserum to an HAV VP4 peptide (provided by D. Sanger) in NTE-40 buffer (50 mM Tris [pH 7.9], 150 mM NaCl, 5 mM EDTA, 0.1% Nonidet P-40). Antigen-antibody complexes were precipitated by the addition of protein A-bearing staphylococcal cells (Pansorbin; Calbiochem) for 90 min at room temperature and then briefly centrifuged. The precipitate was washed with NTE-40 before electrophoresis through a 12% sodium dodecyl sulfate (SDS)-polyacrylamide gel. The gel was fixed, soaked in En^{3}Hance (DuPont) before drying, and exposed overnight to X-Omat AR film (Eastman Kodak). Separate

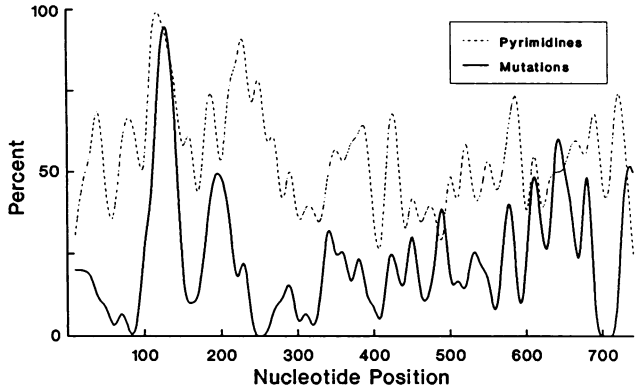

FIG. 2. Frequency of pyrimidine residues and mutations from the HM175 5′NTR sequence in eight other strains of HAV. The primary sequence data are shown in Fig. 1. The percentage of pyrimidine residues was calculated for windows of 10 base positions. Also shown is the frequency with which individual base positions demonstrated substitutions, deletions, or insertions, calculated for windows of 10 bases. Although mutational frequency was generally greatest within the 5′ half of the 5′NTR, this trend was underestimated since the complete 5′NTR sequence, extending to the 5′ terminus, was available for only five virus strains.

aliquots of the labeled translation products were not immunoprecipitated prior to electrophoresis but were otherwise treated similarly.

Nucleotide sequence accession numbers. The GenBank accession numbers for the 5′NTR nucleotide sequences of CF53 and PA21 are M63025 and M63026, respectively.

RESULTS

Sequence heterogeneity within the HAV 5′NTR. We determined the 5′NTR sequences of the genetically divergent PA21 and CF53 strains (Fig. 1). Although the nucleotide sequences of these viruses differ from that of HM175 by up to 25% within the P1/P2 junction region (21), the 5′NTRs of PA21 virus (bases 60 to 734) and CF53 virus (bases 75 to 734) differed from HM175 at 11 and 7.4% of base positions only. Because of this high degree of conservation, the alignment of these 5′NTR sequences with those of seven other human and simian viruses was straightforward except within a lengthy pyrimidine-rich tract present between bases 99 and 142 of wild-type HM175 virus (Fig. 1). Compared with the sequence of HM175 virus (7), the PA21 strain had a 13-base deletion in this region, while CF53 virus had an overlapping 14-base deletion. We examined the sequence alignment for the presence of nucleotide base substitutions, deletions, and insertions and calculated for a window of 10 bases the frequency of base positions at which mutations from the wild-type HM175 sequence occurred in other strains (Fig. 2). This simple analysis revealed the presence of three highly conserved regions (bases 66 to 95, 227 to 262, and 681 to 721) as well as the highly variable pyrimidine-rich tract.

Predicted 5′NTR secondary structure. The alignment permitted the identification of covariant substitutions predictive of conserved helical structures within the 5′NTR (Table 2) (17). These conserved potential base pairs were included as folding constraints on the prediction of the 5′NTR secondary structure by the RNAFOLD program. Inasmuch as the majority of covariant substitutions occurred downstream of base 331, the model structure generated by this analysis is more likely to be correct in the 3′ half of the 5′NTR.

TABLE 2. Conserved 5′NTR nucleotide base pairs predicted by covariant substitutions

Helix[a]	Conserved base pairs[b]
IIId	185–195, 186–194, 187–193
IVb	331–577, 333–575, 336–572, 345–563[c]
IVe	386–526
IVg	418–443, 419–442, 420–441
IVh	428–434
IVi	447–521, 454–513
IVj	463–501
Va	600–679, 601–678, 602–677
Vc	618–638, 619–637, 620–636, 621–635
Vd	646–660, 647–659, 648–658, 649–657

[a] Helical segments listed by major domain (see Fig. 1 and 3).
[b] Wild-type HM175 base positions.
[c] Nuclease studies suggested that A-563 is in a single-stranded domain.

Modifications in the predicted structure, particularly in the 5′ half of the model, were made on the basis of the results of a similar analysis with the STAR program. Where the RNAFOLD and STAR programs generated conflicting predictions, the choice of final structure was based on the likelihood that the predicted structure would be conserved despite variations in the nucleotide sequences of the nine different HAV strains, as well as the identification of single- and double-stranded regions based on the site-specific cleavage of synthetic RNAs by different nucleases. The resulting model of the 5′NTR structure (Fig. 3) thus represents the combined results of a search for nucleotide substitutions predictive of or at least permissive for conserved helices, thermodynamic predictions, and experimental analysis with single-strand-specific (T_1, T_2, and S1) and double-strand-specific (V_1) RNase probes.

The resulting model structure suggested that the 5′NTR contains two highly folded regions (bases 1 to 94 and 155 to 734) separated by a single-stranded region (bases 95 to 154) containing the highly variable pyrimidine-rich segment (Fig. 3). The segment from 99 to 124 of the HM175 5′NTR represents a true polypyrimidine tract. The extensive sequence heterogeneity present in the pyrimidine-rich tract between bases 113 and 132, which was without evidence of mutational covariance (Fig. 1 and 2), suggested that this region is not involved in the formation of conserved helical structures. This view is consistent with the fact that the pyrimidine content of the HAV 5′NTR (402 base residues in HM175 virus) significantly exceeds the purine content (332 base residues) (Fig. 2).

The final model structure contains six major secondary structure domains, labelled I through VI beginning at the 5′ terminus of the 5′NTR (Fig. 3). Domains I and II have a relatively conserved primary structure (Fig. 1 and 2). Domain I (bases 1 to 41) is likely to form a large hairpin structure at the extreme 5′ end of the genome (7), analogous to that found in other picornaviruses (26). The structure of domain II (bases 42 to 98) is less certain, because the absence of sequence variability (Fig. 1) precluded the identification of covariant mutations and we did not determine nuclease sensitivity in this region. The STAR program predicted only one of two possible pseudoknots in domain II (Fig. 3). With the exception of a series of covariant mutations (Table 2) that serve to fix the existence of a single stem-loop, the structure of domain III (bases 99 to 323) was poorly defined. RNAFOLD and STAR programs predicted different structures in this region; that which is shown in Fig.

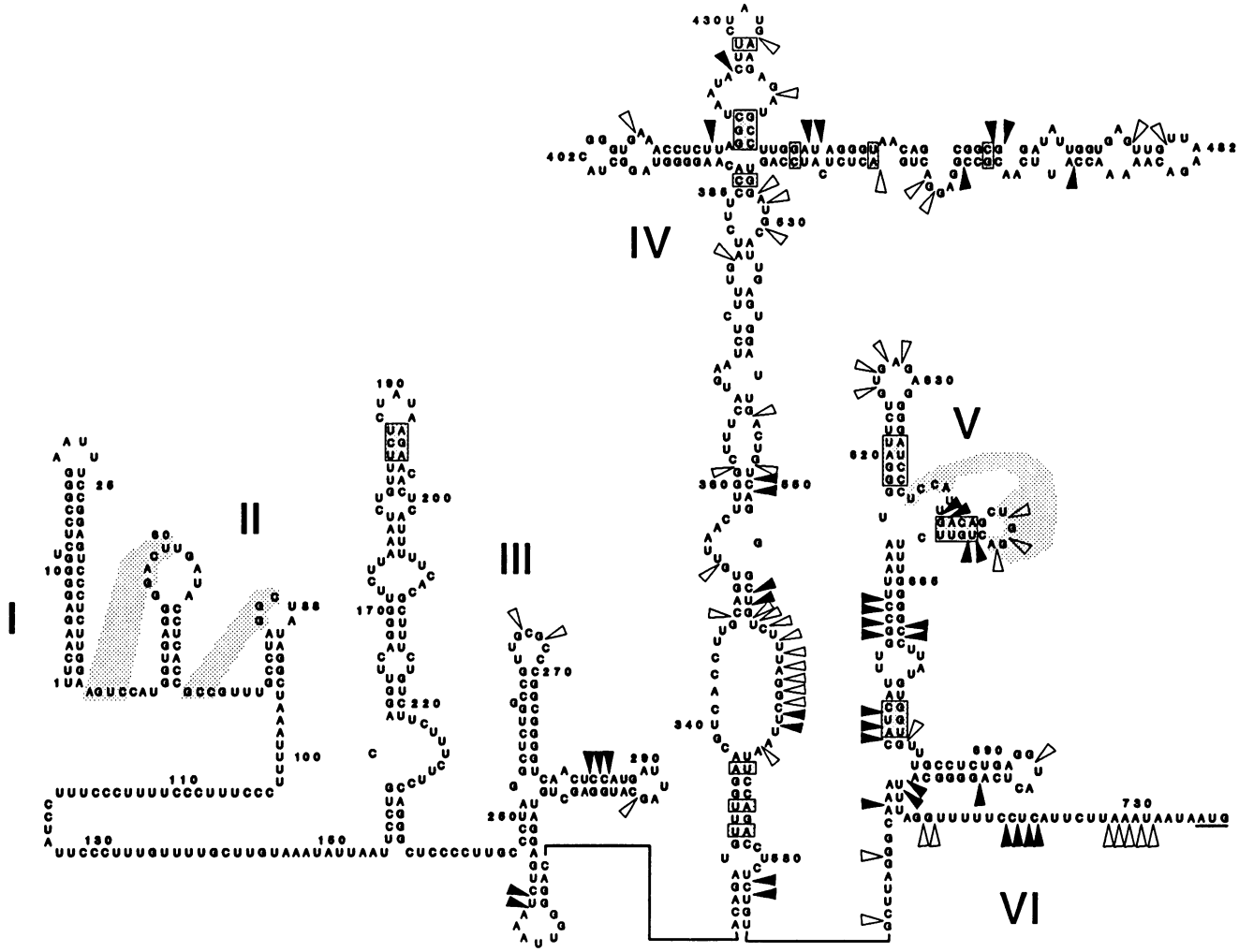

FIG. 3. Proposed secondary structure for wild-type HM175 5'NTR RNA. Boxes delineate the sites of covariant nucleotide substitutions upon which the model is based. Solid arrows indicate sites of cleavage with double-strand-specific RNase (V_1); hollow arrows indicate sites of cleavage with single-strand-specific RNase (S1, T_1, or T_2). Shaded areas indicate potential pseudoknot interactions. Major domains are labelled I through VI. The putative initiator codon (AUG-11) is underlined.

3 reflects the STAR program output with modifications suggested by the results of the enzymatic analysis. The region between bases 203 and 250 is particularly pyrimidine rich (83%) (Fig. 2).

Most of the covariant substitutions identified in the 5'NTR (Table 2) occurred in two large stem-loop structures which comprise domains IV and V, between bases 324 and 692 (Fig. 3). It is thus likely that these are the most accurate components of the model structure. Domain IV has a long stem with multiple internal loops and a cloverleaf structure near the apex which is well defined by covariant substitutions in multiple HAV strains (Fig. 4). The helix which constitutes the lower part of this major stem was defined by three pairs of covariant nucleotide substitutions. Enzymatic analysis in this region was consistent with the proposed structure (Fig. 3). However, the central section of this domain (bases 338 to 387 and 525 to 570) does not contain conserved helical structures predicted by two or more pairs of covariant substitutions. The structure shown in this region is thus derived from thermodynamic predictions and the results of the nuclease digestions, and it may vary somewhat among different virus strains. A large open loop in this stem is predicted by sensitivity to single-strand-specific RNases between bases 557 and 566, despite the existence of covariant substitutions suggesting base pairing between U-345 and A-563 (Table 2). Single-strand-specific RNases did not cause cleavage within the opposite side of this loop (bases 338 to 347), suggesting that it might have a more internal location within the three-dimensional structure of the RNA, making it inaccessible to nucleases, or that it might be base paired to some other, unidentified segment of RNA.

Domain V contains several long helices and a branching stem-loop that may form a pseudoknot between bases 640 and 660 (Fig. 3). The locations of double- and single-strand-specific nuclease cleavage sites provide strong supporting evidence for the helical structures predicted by covariant substitutions in this domain. However, the pseudoknot structure was not confirmed by the enzymatic analysis, which suggested that bases 652 to 655 (UGGA) were not involved in helix formation (Fig. 5). Domain VI extends from the base of the main stem of domain V (U-706) to AUG-11, which opens the reading frame, and includes most of an

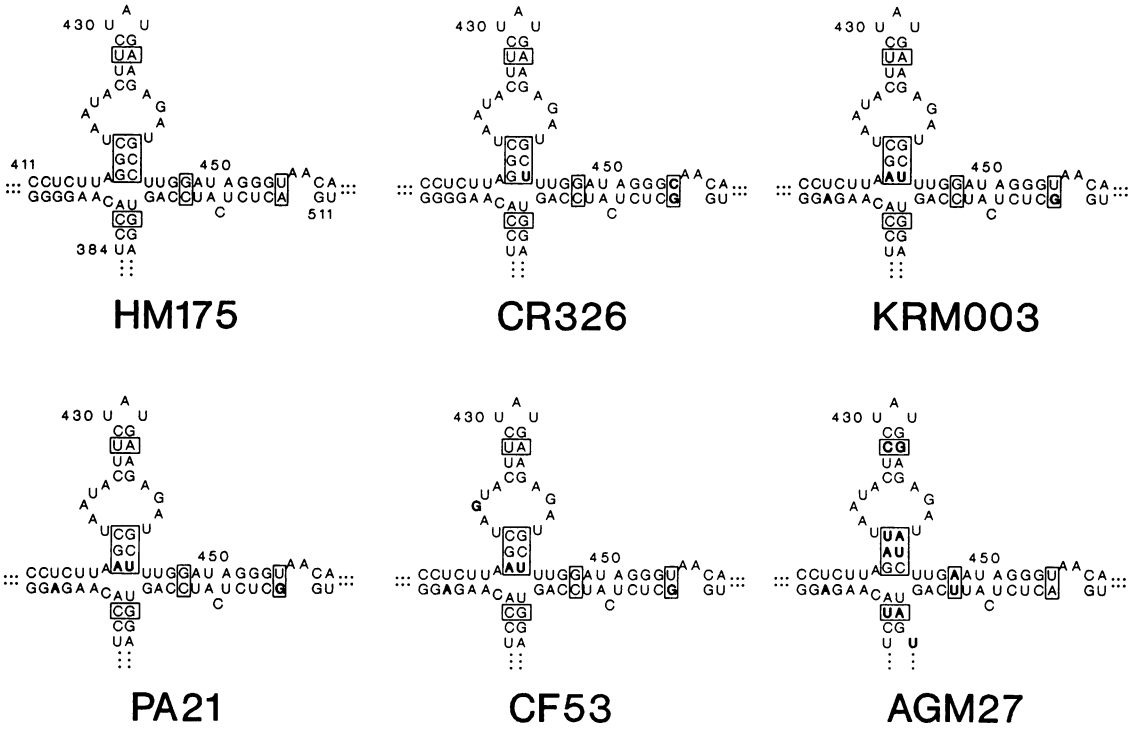

FIG. 4. Primary nucleotide sequence of the domain IV cloverleaf in six HAV strains. Nucleotide substitutions in specific virus strains (from the wild-type HM175 sequence) are shown in boldface type; base pairs identified by covariant substitutions among all nine strains are indicated by boxes.

absolutely conserved 35-base region spanning bases 688 to 722. This region is notable for a short oligopyrimidine tract between bases 713 and 721. Nuclease sensitivity studies suggested that the 3′ end of this oligopyrimidine tract is double stranded (Fig. 3), but the sequence alignment did not allow development of a model conserved structure in this region. It is possible that these bases interact with sequences downstream of the initiating AUG-11, which we did not examine.

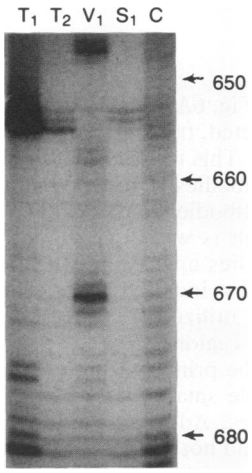

FIG. 5. PAGE of primer extension products derived from synthetic p16 HM175 virus RNA following treatment with single-strand (T_1, T_2, and S1)- or double-strand (V_1)-specific RNases. C denotes the control reaction (no RNase). The region studied is that involving the potential pseudoknot in domain V. Base positions are numbered to the right.

Elements of the HAV 5′NTR controlling translation in vitro. To evaluate the roles that various regions of the HAV 5′NTR play in translation initiation, we constructed a series of plasmids containing cDNA representing the 5′NTR of p16 HM175 virus (20) with progressive 5′ truncations. We evaluated the translation efficiency of RNA synthesized from these plasmids in rabbit reticulocyte lysates in vitro. The translation product was a truncated HAV P1 protein, which was analyzed by SDS-polyacrylamide gel electrophoresis (PAGE) before (Fig. 6A) and after (Fig. 7) immunoprecipitation with antibodies raised to a synthetic peptide representing VP4 or to recombinant VP0. A comparison of the gels shown in these figures indicates that the majority of the translated products could be specifically precipitated by these antibodies. Preliminary experiments demonstrated that the amount of RNA included in the translation reaction mixtures (200 μg/ml) was in excess of that required to achieve maximum translation of the correct product with the full-length message (data not shown). While the RNA used in these experiments represented the 5′NTR of the cell culture-adapted p16 HM175 variant (20), no differences were noted in the translation of this RNA and wild-type HM175 RNA in preliminary experiments (data not shown).

Removal of the first 45 bases of the 5′NTR (pΔ46; Fig. 6A and 7, lanes 2) reduced translation only slightly compared with full-length, control RNA, while further removal of the next 309 bases, a region which includes domain II, the large polypyrimidine tract, and the stem-loop structures proposed for domain III (pΔ355; Fig. 6A and 7, lanes 4), had little additional effect on translation. These data suggest that these structures play little role in controlling translation in vitro.

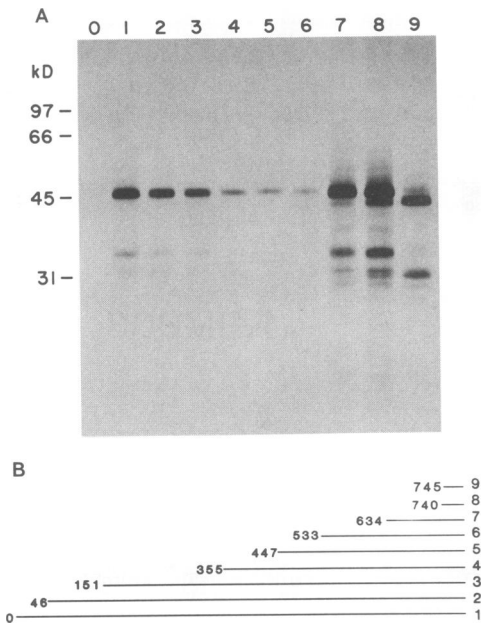

FIG. 6. Products of in vitro translation of synthetic RNAs with progressive 5′ deletions (coding region from bases 735 to 2025). Translation products were not precipitated with specific antibodies prior to gel electrophoresis. (A) Lanes: 0, no RNA control; 1, full-length 5′NTR of HAV (pAccI); 2 to 9, RNAs transcribed from pΔ46, pΔ151, pΔ355, pΔ447, pΔ533, pΔ634, pΔ740, and pΔ745, respectively. Representation of synthetic RNAs used for programming in vitro translation. RNA transcribed from pΔ740 lacks AUG-11; RNA from pΔ745 lacks both AUG-11 and AUG-12.

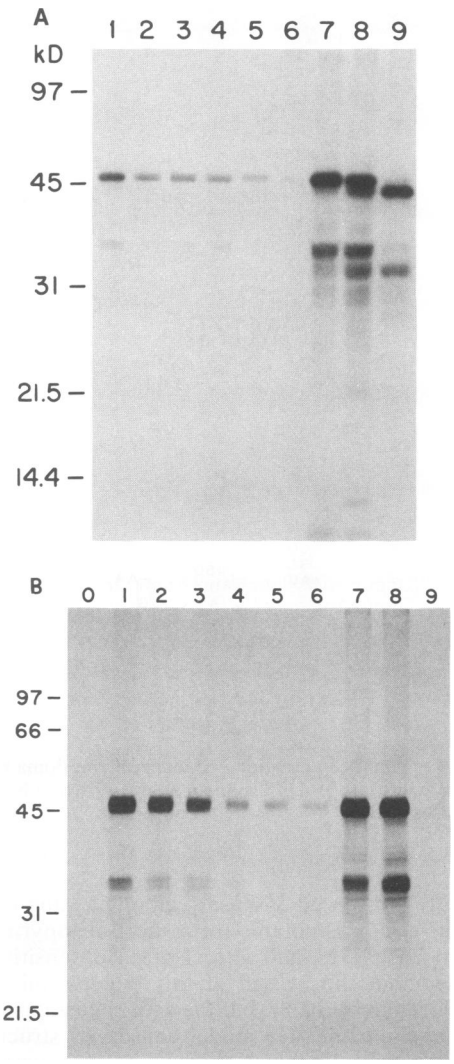

FIG. 7. Analysis of translation products that were immunoprecipitated with antibodies to recombinant VP0 (A) or a VP4 peptide (B) prior to separation by SDS-PAGE. Lanes are labelled as in Fig. 6A.

Removal of another 92 bases to nucleotide 447 (pΔ447; Fig. 6A and 7, lanes 5), which eliminates one-half of the cloverleaf structure within domain IV, reduced translation significantly. Further deletions to nucleotide 533 (pΔ533; Fig. 6A and 7, lanes 6), removing the last arm of the cloverleaf, almost completely abolished translation. However, translation increased to greater than that observed with full-length RNA after an additional deletion to nucleotide 634 (domain V, pΔ634; Fig. 6A and 7, lanes 7). The marked increase in translation observed with RNA from construct pΔ634 is most likely due to an alternative mechanism of initiation utilized by this truncated RNA (see Discussion).

The HAV large open reading frame initiates with two in-frame AUG codons at positions 1 and 3 (AUG-11 and AUG-12 within the complete HAV HM175 sequence). Removal of the first AUG of the long open reading frame did not visibly affect the primary 48-kDa translation product, as the pΔ740 construct translated as efficiently as did pBamHI (Fig. 6A and 7, lanes 8). However, enhanced translation of a slightly smaller secondary product was evident with this construct. The larger product translated from pΔ740 RNA represents translation initiation at the second in-frame AUG-12 (codon 3), as this would lead to a minimally smaller product that could not be distinguished from the full-length protein. The second, visibly smaller translation product most likely represents initiation at the third downstream in-frame AUG codon, AUG-13, which is codon 30 within the open reading frame. The shift to enhanced translation of this secondary product following removal of AUG-11 suggests that the site of initiation with RNA from pΔ634 is in fact AUG-11 and not AUG-12 (see Discussion). RNA from construct pΔ745 (Fig. 6A, lane 9), in which both AUG-11 and AUG-12 were deleted, translated almost as well as did pΔ634 and pΔ740 RNAs. This translation product was immunoprecipitated with antibodies to recombinant VP0 (Fig. 7A, lane 9) but not with antibodies to the HAV VP4 peptide (Fig. 7B, lane 9). This result is what one would expect, as the VP4 peptide sequence lies upstream of AUG-13. The size of the translation product indicates that RNA from construct pΔ745 exclusively utilized AUG-13, which is located within the VP2-encoding region.

In addition to the primary, full-length translation product of 48 kDa, multiple smaller polypeptides were produced in reticulocyte lysates. Addition of HeLa, BS-C-1, or HepG2 cell extracts (11) did not alter this pattern on SDS-polyacrylamide gels (data not shown). All but two of these shorter products were immunoprecipitated by both anti-VP0 (Fig. 7A) and anti-VP4 (Fig. 7B) antibodies, and they were present in amounts correlating with the quantity of full-length product. As the VP4 antibody would precipitate only products initiated within the first 18 residues of the polyprotein

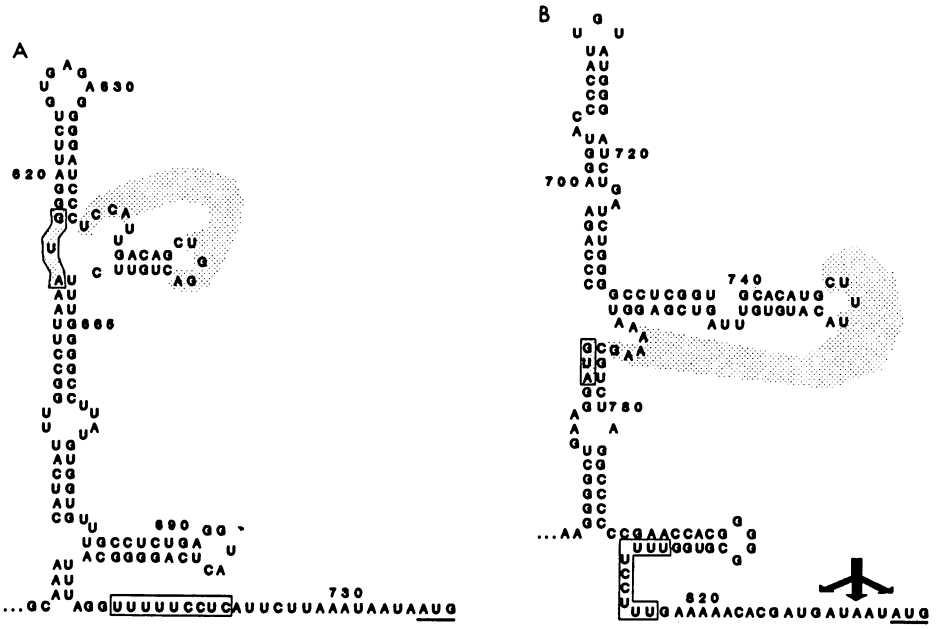

FIG. 8. Comparison of structures proposed for HAV domain V (A) and EMCV domain 4 (B) as proposed by Pilipenko et al. (36). The conserved oligopyrimidine tracts are demarcated by boxes; the conserved internal AUGs are indicated by shaded boxes. Shaded interactions between bases indicate potential pseudoknots.

(assuming that at least 5 residues are needed for immunoreactivity), these results indicate that these products represent premature termination of translation. The two bands seen only in the gel containing nonimmunoprecipitated products (compare Fig. 6A and 7A) likely represent translation products of other reading frames and were not examined further.

DISCUSSION

Several recent reports have documented the existence of considerable nucleotide sequence heterogeneity among different human and nonhuman primate strains of HAV (21, 40). In this report, we describe the nucleotide sequences of the 5′NTRs of two genetically divergent strains (PA21 and CF53). When we aligned these sequences with those of two other recently characterized virus strains (KRM003 and AGM27) and previously published 5′NTR sequences of five other HAV strains, we were able to identify a number of covariant nucleotide substitutions predictive of conserved RNA secondary structures. These covariant substitutions formed the basis for a model of the secondary structure of the HAV 5′NTR, which was further refined by thermodynamic predictions and the results of experiments which examined the effects of single- and double-strand-specific RNases on synthetic RNA.

The most important conclusion to be derived from this work is that the 5′NTR of HAV appears to have a general organization like that of other picornaviruses. In particular, the HAV 5′NTR contains several features which are similar to elements of structural models proposed for the 5′NTRs of the cardioviruses and aphthoviruses (36). These features include a series of extreme 5′ stem-loop structures with potential for pseudoknot formation (domains I and II in Fig. 3), as first suggested by Pleij using the STAR program (37a). A high degree of sequence conservation among HAV strains within domain II precluded confirmation of these helical structures by the phylogenetic approach, and we did not examine the sensitivity of this region to nucleases. Thus, this part of the proposed structure remains largely hypothetical. It is noteworthy, however, that the two stem-loops with pseudoknots proposed for domain II involve only conventional Watson-Crick base pairing and do not invoke noncanonical G · U base pairs (Fig. 3). The proposed structure is very different from that which Andino et al. (2) have proposed for the 5′ terminus of poliovirus RNA. Immediately 3′ of the HAV domain II is a polypyrimidine tract; a similar tract is present in the EMCV 5′NTR. There is extensive sequence microheterogeneity within the polypyrimidine tract among HAV isolates. The lack of conservation evident in this region suggests that it does not participate in stable, base-paired structures.

The remainder of the proposed HAV structure, particularly domains IV and V (Fig. 3), is well supported by covariant nucleotide substitutions and the results of the nuclease studies. The structural analogy with the 5′NTR of EMCV is preserved in this region as well. Domain IV in the HAV model and the region defined by Pilipenko et al. (36) as domain 3 in cardioviruses and aphthoviruses each have long stems with multiple bubbles which end in complex cloverleaf structures. Immediately 3′ of this structure in each virus is a second major domain which contains a branching stem-loop. This branching stem-loop contains a shorter helix in HAV than in EMCV (Fig. 8), Theiler's murine encephalomyelitis virus, or foot-and-mouth disease virus (36), but in each of these viruses the nucleotide sequence within the terminal loop is complementary to that within a bubble at the base of the stem, suggesting the possibility of a pseudoknot structure that is conserved across these picornavirus genera (as shown for HAV in Fig. 3). It is important to note, however, that the results of the enzymatic analysis do not support the existence of this pseudoknot (Fig. 5). Also notable is the presence of a conserved AUG within the strand opposing the base of this helix (bases 615 to 618 in HAV HM175; Fig. 7).

This domain is followed by a short oligopyrimidine tract (domain VI). The nucleotide sequence is absolutely conserved among the nine HAV strains within this region (Fig. 1). The oligopyrimidine tract (bases 712 to 723) is similar in sequence and location to an oligopyrimidine tract near the 3′ terminus of the EMCV 5′NTR. In HAV, it precedes the presumed AUG start codon by a highly variable stretch of only 3 to 11 bases. We are uncertain of the secondary structure assumed by the oligopyrimidine tract in HAV but suspect that it is involved in a stable base-paired structure on the basis of its susceptibility to cleavage by cobra venom RNase (V_1) between bases C-716 and C-720 (Fig. 3).

The similarities in the apparent secondary structure of the HAV and EMCV 5′NTRs (Fig. 8) are consistent with the fact that HAV, although sharing little sequence homology with viruses from any other picornaviral genera, is somewhat more closely related to the cardioviruses (7). The structural similarities suggest that the 5′NTRs of these viruses have analogous functions. In EMCV, the region from bases 403 to 815 constitutes an IRES element which directs internal binding of the 40S ribosomal subunit and is required for initiation of cap-independent translation (19). While the in vitro translation studies that we describe in this report do not directly demonstrate an IRES element in the HAV 5′NTR, our results are consistent with and predictive of a functionally similar domain.

We found translation of the HAV P1 protein to be little affected by removal of the 5′ 354 bases of the 5′NTR (Fig. 6 and 7). The slight decrease in the amount of product observed following removal of the first hairpin structure (bases 1 to 45) may reflect the involvement of this structure in HAV translation, as shown recently for poliovirus (40). No further decrease was evident until deletion of bases beyond position 354. Removal of the 5′-terminal 446 and 532 bases of the 5′NTR, however, resulted in progressive reductions in the amount of translated P1 product. These results suggest that domain IV is critically involved in formation of an HAV IRES element, the removal of which eliminates cap-independent translation in the reticulocyte lysate which is dependent upon internal ribosomal entry. Further removal of the 5′-terminal sequence (to base 634) restored translation to an amount greater than that observed with the full-length 5′NTR. These observations resemble those of Nicklin et al. (31) concerning poliovirus RNA. We suspect that this enhanced translation represents the result of conventional ribosomal scanning from the 5′ terminus, which occurs independently of the presence of a 5′-terminal m^7G cap in reticulocyte lysates. The contrasting lack of translation observed with RNA which was truncated at base 533 (Fig. 6) suggests that the stable helical structures of the intact domain V present an obstacle to efficient ribosomal scanning. If so, the bulk of translation observed with lengthier 5′NTR constructs must be due to internal ribosomal entry. An increase in the relative amount of translation products initiating at AUG-13, which is downstream in the reading frame within the region encoding VP2, was observed following removal of the entire 5′NTR, including AUG-11 (the first AUG within the HAV open reading frame). This suggests that AUG-11 is the usual initiation codon when translation is mediated by ribosomal scanning from the 5′ terminus. There is still a formal possibility, however, that internal entry may occur within the three bases separating AUG-11 and AUG-12 and that translation in vivo initiates at AUG-12.

Kaminski et al. have suggested that EMCV and poliovirus, although both possessing IRES elements within their respective 5′NTR segments, follow somewhat different translation strategies (22). In the case of poliovirus, ribosomal entry occurs over 150 bases upstream of the initiating AUG codon, and internal entry is followed by progressive 3′ translocation (scanning) of the ribosome. With EMCV, however, there is convincing evidence that ribosomal entry occurs less than 5 to 8 bases upstream of the initiating AUG (22). The close proximity of the conserved oligopyrimidine tract to the initiating codon in the HAV sequence suggests that this may be the case with HAV also. Because the sequence of the AGM27 strain of HAV contains an AUG within a favorable context for initiation of translation (..GUUAUGG..) 46 bases upstream of the putative initiating AUG, ribosomal entry most likely occurs between bases 680 and 741 (numbering based on the wild-type HM175 sequence). Thus, domain V, like domain IV, plays a key role in defining the IRES element of HAV. This is consistent with the notion that this domain is analogous to stem-loop 4 in the EMCV 5′NTR model of Pilipenko et al. (36) (Fig. 8).

At least one and possibly two cellular proteins specifically recognize and bind to the IRES element of picornaviruses (9, 18, 19, 28, 29). These cellular proteins presumably play an important role in controlling internal ribosomal entry. We have shown previously that a mutation at base 687 enhances the growth of the HM175 strain of HAV in continuous cultures of monkey kidney cells (8). This mutation is located within the 3′-terminal stem-loop of the putative HAV IRES element, just 24 bases upstream of the oligopyrimidine tract. Its presence does not affect the in vitro translation efficiency of the 5′NTR in reticulocyte lysates (unpublished data). However, it is possible that the mutation may enhance the interaction between the IRES element and proteins which are specific to monkey kidney cells. The cellular proteins that are putatively involved in cap-independent translation may differ somewhat among specific types of mammallian cells, and mutations within the IRES element may thus reflect changes in the host range of the virus. Additional mutations that have been found to be present in cell culture-adapted HM175 virus variants have been found at bases 152 and 203, upstream or near the probable 5′ limits of the HAV IRES (6, 20, 39). Further studies will be required to learn whether these mutations influence translational competency of the 5′NTR in vivo or promote other important 5′NTR functions such as polymerase recognition or particle assembly.

ACKNOWLEDGMENTS

We are grateful to Y. Moritsugu and A. Nomoto for providing sequence data in advance of publication and to J. Johnston and D. Sangar for antisera. We also appreciate the collaboration with S. Tsarev and the receipt of 300 bases of sequence from the AGM027 5′NTR (shown in Fig. 1) on 26 March 1990 for the purpose of experimentation in our laboratory.

This work was supported in part by grants from the U.S. Army Medical Research and Development Command (DAMD 17-89-Z-9022), The World Health Organization Programme for Vaccine Development, and Merck Sharp & Dohme Research Laboratories.

REFERENCES

1. **Abrahams, J. P., M. van der Berg, E. von Batenburg, and C. Pleij.** 1990. Prediction of RNA secondary structure, including pseudoknotting, by computer simulation. Nucleic Acids Res. **18**:3035–3044.
2. **Andino, R., G. E. Rieckhof, and D. Baltimore.** 1990. A functional ribonucleoprotein complex forms around the 5′ end of poliovirus RNA. Cell **63**:369–380.
3. **Bienkowska-Szewczyk, K., and E. Ehrenfeld.** 1988. An internal

5'-noncoding region required for translation of poliovirus RNA in vitro. J. Virol. **62**:3068–3072.
4. **Brown, E. A., R. W. Jansen, and S. M. Lemon.** 1989. Characterization of a simian hepatitis A virus (HAV): antigenic and genetic comparison with human HAV. J. Virol. **63**:4932–4937.
5. **Cohen, J. I., B. Rosenblum, S. M. Feinstone, J. Ticehurst, and R. H. Purcell.** 1989. Attenuation and cell culture adaptation of hepatitis A virus (HAV): a genetic analysis with HAV cDNA. J. Virol. **63**:5364–5370.
6. **Cohen, J. I., B. Rosenblum, J. R. Ticehurst, R. J. Daemer, S. M. Feinstone, and R. H. Purcell.** 1987. Complete nucleotide sequence of an attenuated hepatitis A virus: comparison with wild-type virus. Proc. Natl. Acad. Sci. USA **84**:2497–2501.
7. **Cohen, J. I., J. R. Ticehurst, R. H. Purcell, A. Buckler-White, and B. M. Baroudy.** 1987. Complete nucleotide sequence of wild-type hepatitis A virus: comparison with different strains of hepatitis A virus and other picornaviruses. J. Virol. **61**:50–59.
8. **Day, S. P., and S. M. Lemon.** 1990. A single base mutation in the 5' noncoding region of HAV enhances replication of virus in vitro, p. 175–178. *In* F. Brown, R. M. Chanock, H. S. Ginsberg, and R. A. Lerner (ed.), Vaccines 90: modern approaches to new vaccines including prevention of AIDS. Cold Spring Harbor Laboratory Press, Cold Spring Harbor, N.Y.
9. **del Angel, R. M., A. G. Papavassiliou, C. Fernandez-Thomas, S. J. Silverstein, and V. R. Racaniello.** 1989. Cell proteins bind to multiple sites within the 5' untranslated region of poliovirus RNA. Proc. Natl. Acad. Sci. USA **86**:8299–8303.
10. **Devereux, J., P. Haeberli, and O. Smithies.** 1984. A comprehensive set of sequence analysis programs for the VAX. Nucleic Acids Res. **12**:387–395.
11. **Dorner, A. J., B. L. Semler, R. J. Jackson, R. Hanecak, E. Duprey, and E. Wimmer.** 1984. In vitro translation of poliovirus RNA: utilization of internal initiation sites in reticulocyte lysate. J. Virol. **50**:507–514.
12. **Evans, D. M. A., G. Dunn, P. D. Minor, G. C. Schild, A. J. Cann, G. Stanway, J. W. Almond, K. Currey, and J. V. Maizel, Jr.** 1985. Increased neurovirulence associated with a single nucleotide change in a noncoding region of the Sabin type 3 poliovaccine genome. Nature (London) **314**:548–550.
13. **Freier, S. M., R. Kierzek, J. A. Jaeger, N. Sugimoto, M. H. Caruthers, T. Neilson, and D. H. Turner.** 1986. Improved free-energy parameters for predictions of RNA duplex stability. Proc. Natl. Acad. Sci. USA **83**:9373–9377.
14. **Gauss-Müller, V., and F. Deinhardt.** 1984. Effect of hepatitis A virus infection on cell metabolism in vitro. Proc. Soc. Exp. Biol. Med. **175**:10–15.
15. **Hahn, C. S., E. G. Strauss, and J. H. Strauss.** 1989. Dideoxy sequencing of RNA using reverse transcriptase. Methods Enzymol. **180**:121–130.
16. **Hewlett, M. J., J. K. Rose, and D. Baltimore.** 1976. 5'-Terminal structure of poliovirus polyribosomal RNA is pUp. Proc. Natl. Acad. Sci. USA **73**:327–330.
17. **James, B. D., G. J. Olsen, and N. R. Pace.** 1989. Phylogenetic comparative analysis of RNA secondary structure. Methods Enzymol. **180**:227–239.
18. **Jang, S. K., M. V. Davies, R. J. Kaufman, and E. Wimmer.** 1989. Initiation of protein synthesis by internal entry of ribosomes into the 5' nontranslated region of encephalomyocarditis virus RNA in vivo. J. Virol. **63**:1651–1660.
19. **Jang, S. K., and E. Wimmer.** 1990. Cap-independent translation of encephalomyocarditis virus RNA: structural elements of the internal ribosomal entry site and involvement of a cellular 57-kD RNA-binding protein. Genes Dev. **4**:1560–1572.
20. **Jansen, R. W., J. E. Newbold, and S. M. Lemon.** 1988. Complete nucleotide sequence of a cell culture-adapted variant of hepatitis A virus: comparison with wild-type virus with restricted capacity for *in vitro* replication. Virology **163**:299–307.
21. **Jansen, R. W., G. Siegl, and S. M. Lemon.** 1990. Molecular epidemiology of human hepatitis A virus defined by an antigen-capture polymerase chain reaction method. Proc. Natl. Acad. Sci. USA **87**:2867–2871.
22. **Kaminski, A., M. T. Howell, and R. J. Jackson.** 1990. Initiation of encephalomyocarditis virus RNA translation: the authentic initiation site is not selected by a scanning mechanism. EMBO J. **9**:3753–3759.
23. **Kozak, M.** 1986. Point mutations define a sequence flanking the AUG initiator codon that modulates translation by eukaryotic ribosomes. Cell **44**:283–292.
24. **Kozak, M.** 1989. The scanning model for translation: an update. J. Cell Biol. **108**:229–241.
25. **Krol, A., and P. Carbon.** 1989. A guide for probing native small nuclear RNA and ribonucleoprotein structures. Methods Enzymol. **180**:212–227.
26. **Larsen, G. R., B. L. Semler, and E. Wimmer.** 1981. Stable hairpin structure within the 5'-terminal 85 nucleotides of poliovirus RNA. J. Virol. **37**:328–335.
27. **Linemeyer, D. L., J. G. Menke, A. Martin-Gallardo, J. V. Hughes, A. Young, and S. W. Mitra.** 1985. Molecular cloning and partial sequencing of hepatitis A viral cDNA. J. Virol. **54**:247–255.
28. **Luz, N., and E. Beck.** 1990. A cellular 57 kDa protein binds to two regions of the internal translation initiation site of foot-and-mouth disease virus. FEBS Lett. **269**:311–314.
29. **Meerovitch, K., J. Pelletier, and N. Sonenberg.** 1989. A cellular protein that binds to the 5'-noncoding region of poliovirus RNA: implications for internal translation initiation. Genes Dev. **3**:1026–1034.
30. **Najarian, R., D. Caput, W. Gee, S. J. Potter, A. Renard, J. Merryweather, G. Van Nest, and D. Dina.** 1985. Primary structure and gene organization of human hepatitis A virus. Proc. Natl. Acad. Sci. USA **82**:2627–2631.
31. **Nicklin, M. J. H., H. G. Kräusslich, H. Toyoda, and J. J. Dunn.** 1987. Poliovirus polypeptide precursors: expression *in vitro* and processing by exogenous 3C and 2A proteinases. Proc. Natl. Acad. Sci. USA **84**:4002–4006.
32. **Nomoto, A., Y. F. Lee, and E. Wimmer.** 1976. The 5' end of poliovirus mRNA is not capped with $m^7G(5')ppp(5')Np$. Proc. Natl. Acad. Sci. USA **73**:375–380.
33. **Omata, T., M. Kohara, S. Kuge, T. Komatsu, S. Abe, B. L. Semler, A. Kameda, H. Itoh, M. Arita, E. Wimmer, and A. Nomoto.** 1986. Genetic analysis of the attenuation phenotype of poliovirus type 1. J. Virol. **58**:348–358.
34. **Paul, A. V., H. Tada, K. von der Helm, T. Wissel, R. Kiehn, E. Wimmer, and F. Deinhardt.** 1987. The entire nucleotide sequence of the genome of human hepatitis A virus (isolate MBB). Virus Res. **8**:153–171.
35. **Pelletier, J., and N. Sonenberg.** 1988. Internal initiation of translation of eukaryotic mRNA directed by a sequence derived from poliovirus RNA. Nature (London) **334**:320–325.
36. **Pilipenko, E. V., V. M. Blinov, B. K. Chernov, T. M. Dmitrieva, and V. I. Agol.** 1989. Conservation of the secondary structure elements of the 5'-untranslated region of cardio- and aphthovirus RNAs. Nucleic Acids Res. **17**:5701–5711.
37. **Pilipenko, E. V., V. M. Blinov, L. I. Romanova, A. N. Sinyakov, S. V. Maslova, and V. I. Agol.** 1989. Conserved structural domains in the 5'-untranslated region of picornaviral genomes: an analysis of the segment controlling translation and neurovirulence. Virology **168**:201–209.
37a. **Pleij, C. W. A.** 1990. Pseudoknots in noncoding regions of viral RNAs. Proc. VIIIth Int. Congr. Virol., p. 49–50.
38. **Rivera, V. M., J. D. Welsh, and J. V. Maizel, Jr.** 1988. Comparative sequence analysis of the 5' noncoding region of the enteroviruses and rhinoviruses. Virology **165**:42–50.
39. **Ross, B. C., R. N. Anderson, P. C. Edwards, and I. D. Gust.** 1989. Nucleotide sequence of high-passage hepatitis A virus strain HM175: comparison with wild-type and cell culture-adapted strains. J. Gen. Virol. **70**:2805–2810.
40. **Simoes, E. A. F., and P. Sarnow.** 1991. An RNA hairpin at the extreme 5' end of the poliovirus RNA genome modulates viral translation in human cells. J. Virol. **65**:913–921.
41. **Skinner, M. A., V. R. Racaniello, G. Dunn, J. Cooper, P. D. Minor, and J. W. Almond.** 1989. A new model for the secondary structure of the 5' noncoding RNA of poliovirus is supported by biochemical and genetical data which also show that RNA secondary structure is important in neurovirulence. J. Mol. Biol. **207**:379–392.

42. **Sonenberg, N.** 1987. Regulation of translation by poliovirus. Adv. Virus Res. **33**:175–204.
43. **Sverdlov, E. D., S. A. Tsarev, S. V. Markova, S. K. Vasilenko, V. E. Chizhikov, N. A. Petrov, Y. Y. Kusov, T. A. Nastashenko, and M. S. Balayan.** 1987. Cloning and expression of hepatitis A virus genome in *E. coli* cells. Mol. Gen. (Life Sci. Adv.) **6**:129–133.
44. **Ticehurst, J. R., J. I. Cohen, S. M. Feinstone, R. H. Purcell, R. W. Jansen, and S. M. Lemon.** 1989. Replication of hepatitis A virus: new ideas from studies with cloned cDNA, p. 27–50. *In* E. Ehrenfeld and B. L. Semler (ed.), Molecular aspects of picornavirus infection and detection. American Society for Microbiology, Washington, D.C.
45. **Trono, D., R. Andino, and D. Baltimore.** 1988. An RNA sequence of hundreds of nucleotides at the 5′ end of poliovirus RNA is involved in allowing viral protein synthesis. J. Virol. **62**:2291–2299.
46. **Trono, D., J. Pelletier, N. Sonenberg, and D. Baltimore.** 1988. Translation in mammalian cells of a gene linked to the poliovirus 5′ noncoding region. Science **241**:445–448.